Acc. Chem. Res. **2002,** *35,* 817−825

Characterization of Nucleic Acids by Nanopore Analysis

DAVID W. DEAMER*
Department of Chemistry and Biochemistry, University of California, Santa Cruz, California 95064

DANIEL BRANTON
Biology Laboratories, Harvard University, Cambridge, Massachusetts 02138

Received October 15, 2001

ABSTRACT

Single-stranded DNA and RNA molecules in solution can be driven through a nanoscopic pore by an applied electric field. As each molecule occupies the pore, a characteristic blockade of ionic current is produced. Information about length, composition, structure, and dynamic motion of the molecule can be deduced from modulations of the current blockade.

The Nanopore Concept

One of the most exciting prospects to emerge recently in chemical research has been that the properties of single molecules can now be investigated. Although single-molecule techniques such as atomic force microscopy can provide valuable information, it is usually necessary for a molecule to be immobilized before it can be probed. In this Account, we will describe a novel analytical approach that permits individual molecules in solution to be drawn into a nanoscopic pore in such a way that their structure, composition, and dynamic properties can be investigated.

We will begin by describing a biological nanopore that was the first to be used successfully in single-molecule analysis of nucleic acids. In the 1970s, it became apparent that biological membranes of cells incorporate a variety of channels composed of proteins. The function of the channels is to provide a gated pore that allows nutrients (glucose, amino acids) and ions (Na^+, K^+, Ca^{2+}, Cl^-) to cross the otherwise impermeable lipid bilayer barrier that surrounds all cells. The fact that such pores could conduct polar and ionic solutes across a membrane inspired us to consider the possibility that certain polymeric solutes might also be translocated through a pore. For instance, if a sufficiently large pore could be embedded in a bilayer, it seemed possible that linear ionic polymers as large as a nucleic acid might be driven through the pore by an applied voltage. Because a nucleic acid molecule would be expected to occupy a large fraction of the pore's volume during translocation, we reasoned that the polymer would transiently reduce, or block, the ionic current created by the applied voltage. Furthermore, if each nucleotide in the polymer produced a characteristic modulation of the ionic current during its passage through the nanopore, the sequence of current modulations would reflect the sequence of bases in the polymer.

A sustained effort by the authors to test this idea began in 1992. The α-hemolysin toxin produced by *Staphylococcus aureus* was identified as a suitable channel because it self-assembles in lipid bilayers to form aqueous pores with diameters just large enough to translocate the nucleotides in a single strand of DNA or RNA. John Kasianowicz at NIST had established conditions in which the hemolysin channel embedded in a lipid bilayer was stable for hours in 1.0 M KCl. In 1993, a research collaboration was undertaken by the authors and Kasianowicz. We soon discovered that addition of a single-stranded nucleic acid homopolymers produced large numbers of transient ionic current blockades, suggesting that individual molecules were being translocated through the pore and blocking ionic current. These results clearly suggested that nucleic acid molecules could, in fact, be drawn through the pore and launched us as aficionados of nanopores for probing DNA and RNA.

Nanopores as Polymer Sensors

The use of nanoscopic pores to investigate macromolecules in solution has attracted increasing interest over the past decade.[1−15] Thus far, only the α-hemolysin channel has demonstrated the necessary properties of continuous nongating conductance and a pore size (1.5 nm) that ensures sequential, single-file translocation of polynucleotide. To produce a nanopore, α-hemolysin subunits are introduced into a buffered solution of 1.0 M KCl that is in contact with a lipid bilayer which separates the solution into two compartments, designated cis and trans. The hemolysin subunits assemble into a heptameric complex that inserts into the cis side of the bilayer to produce a pore that carries an ionic current of approximately 120 pA with an applied voltage of 120 mV. After a single pore and its characteristic current appear, the remaining hemolysin subunits are flushed away to prevent other pores from inserting.

The bilayer and pore are supported at the end of a Teflon tube with a 30 μm hole (Figure 1A). This apparatus, in conjunction with a standard amplifier and software, provides rapid response times in the microsecond range and has substantially lower noise than the larger planar

David Deamer (b. 1939, Santa Monica, CA) attended Duke University (1957−1961, chemistry) and The Ohio State University School of Medicine (Ph.D. 1965). He met Dan Branton during postdoctoral research at UC Berkeley (1965−1967) and began his academic career at UC Davis in 1967. Prof. Deamer moved his laboratory to UC Santa Cruz in 1993. He has held visiting research appointments at the University of Bristol (1971) and the Animal Physiology Institute, Babraham, England (1975), where he studied liposomes, at the Australian National University, Canberra (1985), and the Weizmann Institute, Rehovoth, Israel (1998). His research interests are primarily in membrane biophysics, particularly the self-assembly processes that define biological membrane structure.

Daniel Branton (b. 1932, Antwerp, Belgium) attended Cornell University (B.S. in mathematics) and UC Berkeley (Ph.D. in plant physiology, 1961). Following postdoctoral work in Switzerland, he returned to Berkeley, where he taught from 1963 to 1975. During this time, he established that freeze-fracture electron microscopy reveals the interior structure of biological membranes at molecular resolution. Prof. Branton moved his laboratory to Harvard University in 1976. His research interests have centered on cytoskeletal structures associated with biological membranes. In 1991, Profs. Deamer and Branton initiated research on nanopore analysis of nucleic acids, the topic of the Account described here.

* Corresponding article. E-mail: deamer@hydrogen.ucsc.edu.

10.1021/ar000138m CCC: $22.00
Published on Web 09/27/2002

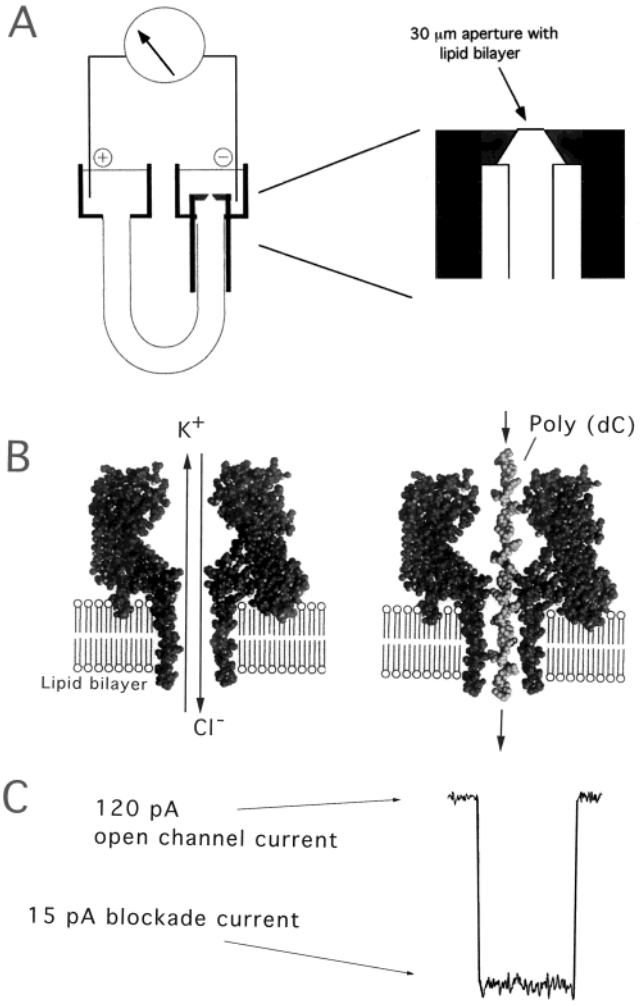

FIGURE 1. (A) Nanopore support device, in which a U-tube supports a lipid bilayer membrane bathed in 1.0 M KCl. Hemolysin subunits are added to the cis chamber facing the bilayer, and a voltage is applied (120 mV) positive on the trans side. When a single pore inserts into the bilayer, a characteristic current of ~120 pA immediately appears. At that point the chamber is flushed so that no further pores can insert. An amplifier with picoampere sensitivity monitors current modulations and sends analog signals to an A/D converter which are stored in a computer for later processing. (B) The hemolysin nanopore is shown in cross section, based on the X-ray data of Song et al.[19] An ionic current of KCl is driven by the applied voltage through the open pore on the left. Under these conditions, ionic polymers such as nucleic acids are captured by the standing electrical field and driven through the pore. A synthetic poly(dC) DNA strand traversing the pore is shown on the right. (C) When a single-stranded nucleic acid molecule traverses the pore, a transient blockade of ionic current results, during which the ionic current is reduced from 120 to 15 pA.

lipid membrane commonly used in single-channel research. Figure 1B illustrates a hemolysin pore in the absence and in the presence of a translocating nucleic acid strand, and Figure 1C shows the resulting blockade produced when a nucleic acid interrupts the flow of potassium and chloride ions through the pore.

Our early experiments suggested that the channel blockades were caused by nucleic acid translocation. Formal proof for this conjecture was the demonstration that the number of blockades was directly correlated with the actual number of nucleic acid molecules that were translocated through the pore.[6] This experiment involved a comparison of the ability of DNA as single-stranded (ssDNA) and double-stranded (dsDNA) molecules to pass through the pore. Quantitative polymerase chain reaction (PCR) was used to make a direct measurement of nucleic acids appearing on the trans side of the membrane, and the numbers were compared with the number of blockade events that occurred during the same time interval. The results were clear and are summarized in Table 1. Only ssDNA appeared on the trans side, while dsDNA remained on the cis side of the pore. The ratio of single-stranded DNA molecules appearing on the trans side to the number of blockade events was close to 1. For instance, in one experiment, 1250 ssDNA molecules appeared on the trans side, and the number of blockades was 1300 in the same time interval.

Table 1[a]

channels in bilayer	blockades per minute	molecules per minute
35	1300	1250
8	220	280
6	150	80

[a] Single-stranded DNA transport quantitatively accounts for pore blockades. The number of blockades per minute is compared with the number of molecules per minute that moved to the trans chamber during experiments in which the cis chamber contained 0.27 mg/mL of 150 nt single-stranded DNA and an equivalent amount of 100 nt double-stranded DNA as an internal control for leaks or aerosol contamination. The number of molecules per minute transported to the trans chamber was calculated from the total number of molecules in the trans chamber measured by competitive PCR analysis and approximately matches the number of blockades per minute. To have sufficient oligonucleotides for PCR amplification, this experiment required multiple channels to be inserted into the bilayer. Their numbers were estimated from the known single-channel current under standard conditions.

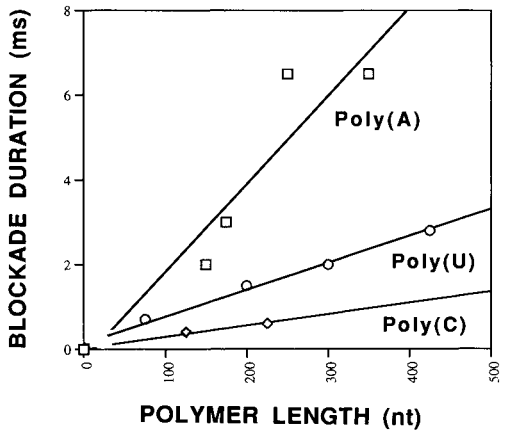

FIGURE 2. Relation between polynucleotide strand length and mean lifetime of ionic current blockades for polyA, polyU, and polyC.

A corollary of this experiment is that for blockades caused by the transport of linear polynucleotides through the pore, blockade lifetimes should be proportional to the length of the polymer. Results for full blockades exhibited by polyU, polyC, and polyA are plotted in Figure 2. All three homopolymers exhibited a linear relation between chain length and duration of the blockade. For RNA molecules, the fastest is polyC (~2 μs/base), poly A is

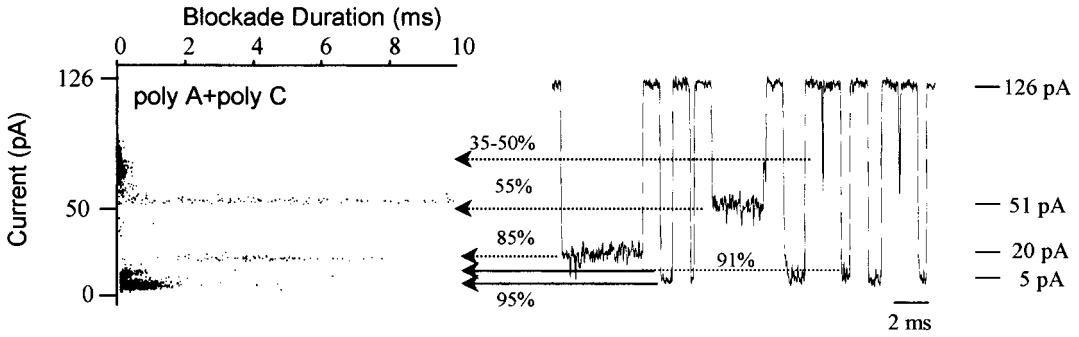

FIGURE 3. Blockades caused by a mixture of polyA (175 nucleotide (nt) nominal length) and polyC (125 nt nominal length). Each point on the event diagram on the left represents a single RNA molecule traversing the pore. The blockades of polyA (55% and 85%) are relatively long and are readily distinguished from the shorter polyC blockades (91% and 95%). The 55% blockades of polyA reflect molecules that enter but do not traverse the pore. The much shorter 35−50% blockades are probably due to RNA molecules colliding with the pore without entering it.

slowest (~20 μs/base), and polyU is intermediate (6 μs/base). The fact that we can readily observe differences in translocation velocities not only between a purine and a pyrimidine homopolymer, but also between two pyrimidine homopolymers, or between poly A and poly dA,[8] provided early encouragement for the notion that a nanopore could distinguish among different molecular species.

Purine and Pyrimidine Polynucleotides Cause Measurably Different Blockade Amplitudes

Akeson et al.[8] investigated blockades of ionic current caused by homopolymers of RNA. The blockade duration and amplitude can be presented as a two-dimensional event diagram in which each point represents a blockade event caused by the passage of a single molecule of RNA through the nanopore (Figure 3). On the right are shown typical examples of the blockade events from which the plots were produced. The pattern of blockades caused by polyC was easily distinguished from the pattern for polyA, whether the polymers were examined separately or in the mixture illustrated in Figure 3. That is, the channel current was reduced significantly more by polyC RNA (typically 95% blockades) than by polyA RNA (85% blockades), and the polyC blockades were significantly shorter in duration compared to polyA. The lower amplitude blockades (~55%) that were relatively common with polyA RNA are due to molecules entering but not being translocated through the pore.

The fact that polyA and polyC could be distinguished by the nanopore suggested that a transition from polyA to polyC segments within a single RNA molecule should be detectable. We therefore synthesized an RNA with the sequence $A_{(30)}C_{(70)}Gp$, which would be expected to produce a bilevel blockade. Such blockades were commonly observed (Figure 4) and interpreted to represent an initial blockade by polyC RNA (current reduced to 5% of open-channel value) followed by polyA RNA (current reduced to 16% of open-channel value).

The evidence presented by Akeson et al.[8] provided the first demonstration that modulations of ionic current during translocation of a macromolecule through a pore

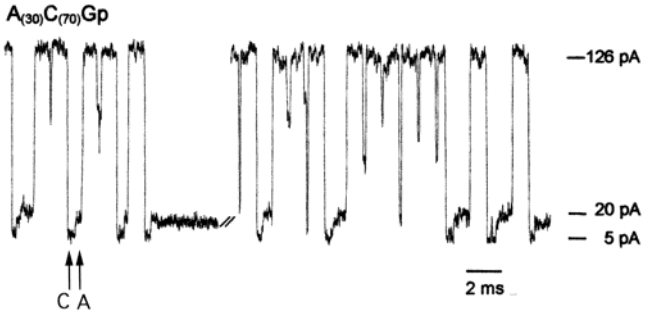

FIGURE 4. Typical blockades caused by $A_{(30)}C_{(70)}Gp$ RNA added to the cis bath at 100 μg mL^{-1}. Each event represents translocation of a single RNA molecule through the pore. Most bilevel events had 5 pA residual current (95% current blockade) followed by a 19 pA residual current (84% blockade). This signal corresponds to the polyC segment at the 3′ end of the molecule entering the pore first.

can be used to discriminate between components along its linear sequence. At first, the greater blockade amplitude associated with polyC was puzzling, because adenine (a purine) is a larger base than cytosine (a pyrimidine). If the size of individual nucleotides within the RNA strands alone dictated blockade amplitudes of ionic current, the polyA might be expected to have had a greater effect. However, earlier reports showed that polyC forms a single-stranded helix with a 1.34 nm diameter,[17] while polyA forms a single-stranded helix with a diameter of 2.1 nm.[18] It therefore seems likely that the smaller polyC helix can readily translocate through the 1.5 nm limiting aperture of the pore, while polyA penetrates the pore only when the helical strand is partially unwound into an extended configuration. The additional energy required to unwind the purine bases is consistent with the significantly longer blockade duration associated with polyA strands. An extended polyA strand would also permit more ionic current to pass during a blockade, which is consistent with our observations. This interpretation also explains why the oligoC portion of the $A_{(30)}C_{(70)}Gp$ block copolymer typically enters first (Figure 4). That is, the thinner oligoC helix would be expected to act as a leader sequence, with the oligoA segment following afterward.

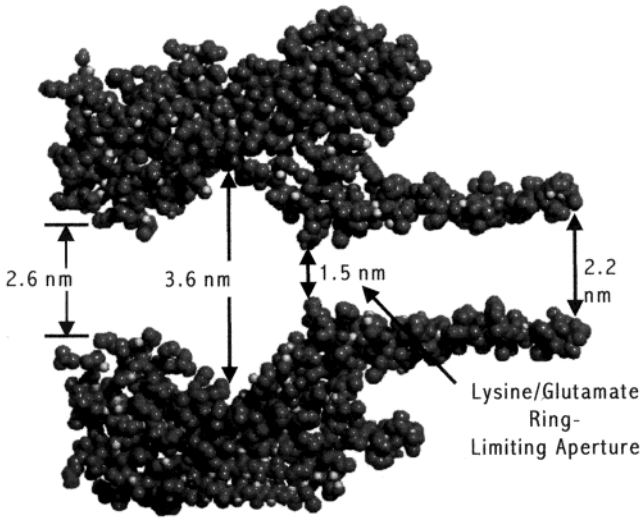

FIGURE 5. Structure of α-hemolysin. This cross section shows the general configuration of the pore, in which seven subunits self-assemble in bilayers to form a heptamer, the stem of which spans the lipid bilayer. The 1.5 nm limiting aperture of the pore is composed of alternating glutamate and lysine residues.

Table 2. Physical Properties of the Aqueous Channel through the Stem of an α-Hemolysin Nanopore

pore internal volume	17.9 nm^3
ions in pore (1.0 M KCl)	11 K^+ and 11 Cl^-
water molecules in pore	~600
ionic current (120 mV)	120 pA
ions passing through pore (120 pA)	7×10^8 s^{-1}
force acting on polymer	~10−20 pN
polymer velocity in pore	0.25−1.7 nm s^{-1}
transit times	1 μs/nt (polydC), 22 μs/nt (polyA)
blockade current (expressed as a fraction of the open-channel value)	polyC, 0.05; polyU, 0.13; polyA, 0.17; polydT abasic polymer, 0.27; polyphosphate, 0.70

What Factors Control Nucleic Acid Movement through the Hemolysin Pore?

Now that we have described some of the basic results of nanopore analysis, we can begin to ask more detailed questions about the mechanism by which ionic current blockades are produced by a nucleic acid molecule in the nanopore. Song et al.[19] reported the crystal structure of α-hemolysin at atomic resolution, and their data were used to prepare the space-filling model shown in Figure 5. The entrance to the channel has a diameter of approximately 2.6 nm that contains a ring of threonine residues. The entry opens into a vestibule with an interior dimension of about 3.6 nm that in turn leads to the pore's stem, which penetrates the lipid bilayer. The average inside diameter of the stem is about 2.0 nm, with a 1.5 nm constriction between the vestibule and the stem. This limiting constriction is composed of alternating lysine and glutamate residues, and the remainder of the stem is lined with neutral amino acids and a single hydrophobic ring of exposed leucine residues. The opening at the other end of the pore has a 2.2 nm ring of alternating lysine and aspartate residues.

Table 2 summarizes physical properties of the pore that are relevant to understanding ionic current blockades. Here we will assume that the major component of the blockade occurs when a nucleic acid occupies the 5 nm long stem of the channel, and we will neglect contributions by the larger vestibule. We obtain the pore volume of 17.9 nm^3 by adding the individual volumes of the 17 rings of amino acids that line the stem. These range from five rings of glycine with a diameter of 2.6 nm, to a single ring of leucine with 1.6 nm diameter. This is equivalent to an average diameter of 2.0 nm.

Blockade Mechanism

The process by which an ionic current blockade is produced must entail three phases: capture, entry, and translocation. When a voltage of 120 mV is imposed on the pore, the resulting ionic current consists of potassium and chloride ions. If single-stranded nucleic acids are present, a given molecule will occasionally diffuse into a small volume near the mouth of the pore. Active capture by the voltage bias has not been examined in detail, but as the polymer enters the biased region, three outcomes are possible. The first is that the diffusing nucleic acid molecule simply collides with the pore mouth. During this collision, the ionic current may be interrupted for a few microseconds, but the duration and extent of this transient blockade are variable and largely independent of chain length.

The second possibility is that one end of the molecule partially enters the vestibule and remains for periods ranging from tens of microseconds to several milliseconds, after which it either diffuses out of the pore or is drawn completely into the pore stem. While the molecule occupies the vestibule, it causes a partial blockade whose characteristic amplitude is about half that of the full blockade.

The third possibility is that one end of the nucleic acid is drawn completely into the pore stem, where it produces a full blockade with a duration that is a function of chain length. Translocation occurs as a result of electrophoretic force acting on the anionic phosphate groups of the chain. The pore stem is only 5 nm long, but the nucleic acid strand can be up to thousands of nucleotides in length. Experiments with very short polynucleotides show that the electric field acts primarily on the 10−14 phosphate groups within the stem.[20] The resultant force of about 10−20 pN is sufficient to drive the molecule through the pore with velocities that depend on the composition and secondary structure of the strand. Given the small aperture of the pore (1.5 nm), the polynucleotides must move as an extended linear polyanion.

Measurable Parameters of Ionic Current Blockades

Three parameters provide information about the nature of the linear polymer passing through a nanopore. The first is blockade amplitude, which is normalized and expressed as a fraction or percentage of the open-channel current, I/I_o, where I is the blockade current and I_o is the open-channel current. I/I_o has a characteristic value for

many homopolymers of RNA and DNA, suggesting that it will be an important analytical feature of nanopore technology.

Blockade duration is the time required for a polymer to pass through the pore. Typical values at 120 mV for different homopolymers range from ~1 μs per nucleotide monomer for oligo(dC) to ~20 μs per nucleotide monomer for oligoA RNA. Blockade signature is defined as a measurable variation in blockade amplitude during translocation. When all three variables are taken into account, the pattern of blockades is different for virtually every linear polymer, again suggesting that nanopore analysis of polymers will provide information never before possible to obtain.

Although several factors could conceivably contribute to blockades of ionic current, the simplest to test experimentally is that the fractional volume of a linear nucleic acid strand occupying a pore will reduce the number of ions available to carry current. The role of fractional volume has been tested by investigating blockades produced by several polyanions that vary in molecular volume, yet have approximately the same charge density of phosphate along the strand. These blockade amplitudes were then compared with the fractional volume of the pore stem occupied by the polymer, taking into account not only the molecular volume of the polymer but also water of hydration on the polymer and pore walls. The exact conformation of a single strand of DNA in the channel is unknown, but for the purposes of this calculation a minimal estimate is 0.34 nm per base, the repeat distance of bases in a double helix. About 15 nucleotides would then be in the pore at any instant. (The pore is defined here as the portion of the hemolysin channel that penetrates the lipid bilayer, and does not include the larger volume of the vestibule and channel mouth.) We assume that each monomer of the nucleic acid has four waters of hydration (60 total), and that a single layer of water is bound to the interior surface of the pore (320 total). With these assumptions, 70% of the available pore volume would be occupied by a single strand of oligo(dA).

Similar calculations were made for oligo(dC), for an abasic strand of nucleic acid, and for polyphosphate, all of which produce measurable ionic current blockades. A plot of blockade amplitude vs fractional molecular volume occupied by the four different polymers shows that blockade amplitude is proportional to the fractional pore volume occupied by a translocating polymer (Figure 6). The experimental values are generally somewhat larger than the calculated values, suggesting that the other factors may play minor roles in contributing to the blockade amplitude. One such possibility is that chloride ion conductance is substantially decreased when the pore is occupied by a negatively charged polymer strand.

From the results of this simple experiment, we conclude that blockade amplitude is largely a function of the fractional volume occupied by a linear polymer traversing a nanopore. The difference in total volume between purine and pyrimidine deoxyoligonucleotides in the

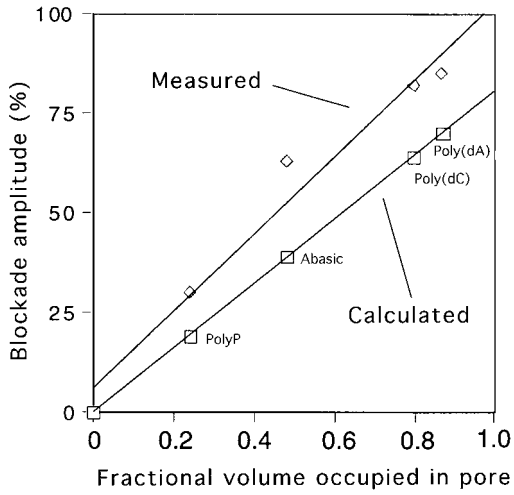

FIGURE 6. Relation between blockade amplitude and fractional volume of a polymer occupying the pore. (See text for details.)

α-hemolysin pore is only 0.3 nm^3, which represents a 6% difference in the volume occupied by the molecules in the pore after correcting for water of hydration. This difference is just barely detectable as an average signal over noise and is produced by multiple nucleotides occupying the length of the pore. Resolution is likely to be improved if synthetic nanopores can be fabricated with limiting apertures that accommodate single, rather than multiple nucleotides.

Nanopore Analysis at Single Base-Pair and Single Nucleotide Resolution

From the measured velocities of single-stranded nucleic acid translocation through the hemolysin pore, it soon became clear that a major factor limiting resolution is the time available to detect current modulation by a single nucleotide. For instance, a single nucleotide in a DNA strand passes through the length of the pore in about 1−2 μs, and in that same time interval only ~100 ions of current comprise the difference between a purine base and a pyrimidine base in the total ionic current of a blockade. Regardless of how perfectly currents can be measured, with so few ions available to measure as current, the measurement precision could not be better than about ±9%. At least an order of magnitude more ions would therefore be required to provide a measurement sufficiently precise to discriminate between single purine and pyrimidine bases as they are translocated through the nanopore.

To demonstrate that larger numbers of ions will permit the sensitivity required for single base resolution, we used DNA "hairpins" to keep a single molecule of DNA in the α-hemolysin channel for relatively long (milliseconds to seconds) time intervals. Hairpins are sequences of single-stranded nucleic acids that fold back on themselves to form hydrogen bonds between Watson−Crick base pairs.[23,24] The entropy and enthalpy components of DNA hairpin formation are readily estimated, and the sequence can be designed so that only intramolecular interactions occur.[25] The expectation was that an exten-

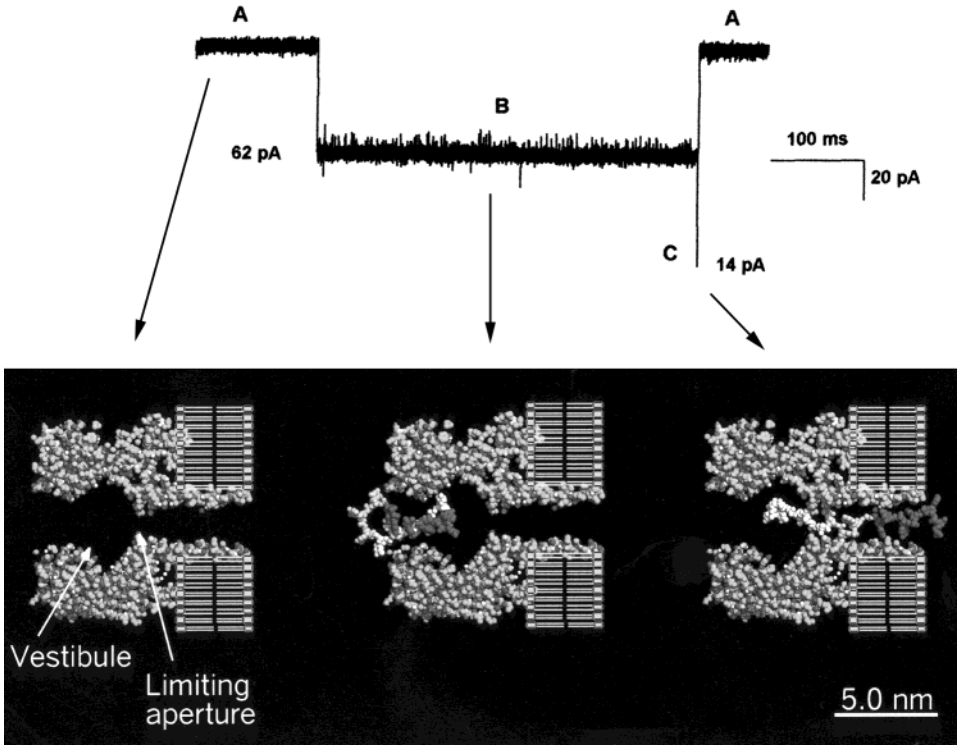

FIGURE 7. Blockade of the α-hemolysin nanopore by a DNA hairpin. The upper panel shows a current trace caused by capture and translocation of a 6 base-pair DNA hairpin through the pore. (A) The 120 mV applied voltage across the open pore produces ~120 pA of ionic current in 1.0 M KCl. (B) Capture of a 6 base-pair DNA hairpin in the channel causes an abrupt current reduction to an intermediate level (I/I_o = 52%, where I is the average event current and I_o is the average open-channel current). Because only linear single-stranded DNA can traverse the 1.5 nm limiting aperture of the pore, the hairpin DNA remains in the vestibule. (C) Translocation of the DNA through the limiting aperture of the channel. The partial hairpin blockade ends with a sharp downward spike to approximately 14 pA (I/I_o = 12%) that lasts about 60 μs. The lower panel shows a molecular model of these events.

sively hydrogen-bonded hairpin structure might enter the vestibule of an α-hemolysin channel but would not be translocated through the pore until all the hydrogen bonds stabilizing the hairpin spontaneously dissociated.

The initial experiments used a well-characterized DNA hairpin with a six-base-pair stem and a four-deoxythymidine loop.[26] When captured within an α-hemolysin nanopore, this molecule caused a partial current blockade (or "shoulder") lasting hundreds of milliseconds (Figure 7, top panel), followed by a rapid downward spike.[14] We interpret this signature as an initial capture of a hairpin stem in the vestibule which produces the shoulder (Figure 7, bottom panel), followed by simultaneous dissociation of the six base pairs in the hairpin stem. The extended single strand can then traverse the pore and produce the spike.

From this result, we concluded that the hairpin blockade reflects current modulation in both the vestibule and the stem of the channel. We went on to analyze a series of blunt-ended DNA hairpins with stems that ranged in length from three to eight base pairs. If the model depicted in Figure 7 is correct, we would expect a substantial increase in blockade shoulder lifetime for each additional base pair and a modest linear increase in the lifetime of the downward spike at the end of the event.

We found that each base pair addition produced a marked increase in median blockade shoulder lifetime

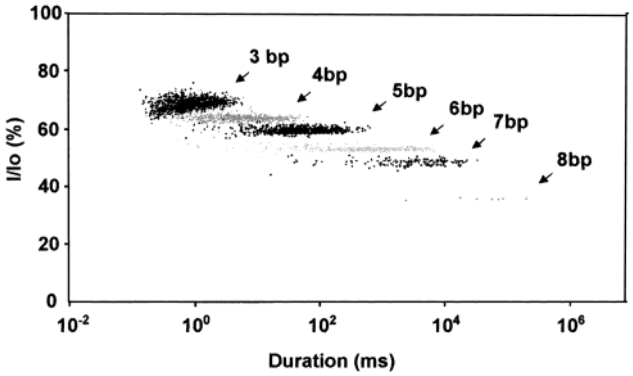

FIGURE 8. Nanopore resolution of single base-pair differences, illustrated as an event diagram for DNA hairpins with 3−8 base-pair stems. Each point represents the duration and amplitude of a shoulder blockade caused by one DNA hairpin captured in the pore vestibule. The duration of the 9 bp hairpin blockade shoulders were too long to record a statistically significant number of events.

(Figure 8). A downward trend in shoulder current amplitude was also observed, from I/I_o = 68% for a 3 bp stem to I/I_o = 32% for a 9 bp stem. These results are consistent with the estimated force acting on the nucleic acid, and they also demonstrate that the nanopore can resolve each additional base pair by the reduction of ionic current as the hairpin stem extends farther into the vestibule.

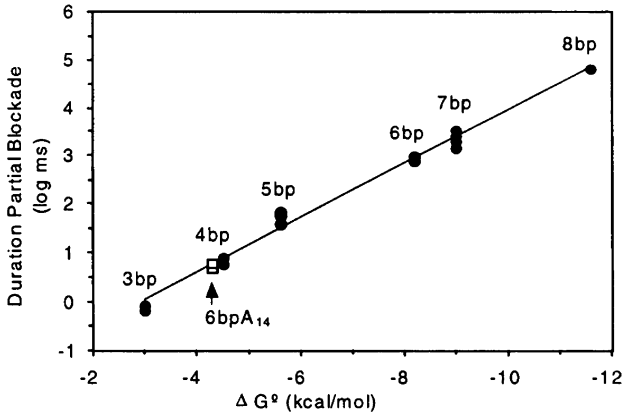

FIGURE 9. Standard free energy of hairpin formation plotted as a function of shoulder blockade duration. All experiments were conducted in 1.0 M KCl at 22 ± 1 °C with a 120 mV applied potential.

Correlation of Blockade Duration with Free Energy of Hairpin Formation

Standard free energy of hairpin formation was calculated and correlated with median duration of hairpin shoulder blockades (solid circles in Figure 9). Each point represents the median blockade duration for a given hairpin length acquired using a separate α-hemolysin pore on a separate day. Median blockade durations and $\Delta G°$ for the equivalent of the 6 bp hairpin with a single mismatch are represented by open squares. The median blockade duration correlated remarkably well with the free energy of formation.

This correlation would not be expected if the force generated by the electric field was simply unzipping the hydrogen-bonded base pairs of the hairpin and drawing the molecule through the pore. Instead, the hairpin remains in the vestibule until all of the hydrogen-bonded complementary bases happen to dissociate simultaneously, at which point the unwound DNA strand is drawn through the pore to produce the spike. The time required before the hairpin dissociates (the shoulder) is an exponential function of the number of base pairs in the hairpin structure and is directly related to the calculated free energy that stabilizes the hairpin. Note that this relation between free energy and blockade duration also extends to a single nucleotide mismatch in the hairpin, in which the AT pair is replaced by an AA pair. This reduces the median blockade duration from ~1 s to 10 ms (open squares, Figure 9), showing that the nanopore can distinguish two DNA molecules that differ by a single nucleotide.

Although these results do not in themselves lead to a method for sequencing, they clearly illustrate the extraordinary ability of a nanopore to provide information about dynamic events occurring in single molecules. Furthermore, they demonstrate that ionic current blockades are sufficient to detect differences between DNA molecules at the single base pair level, suggesting that a suitable nanopore will be able to resolve individual nucleotides.

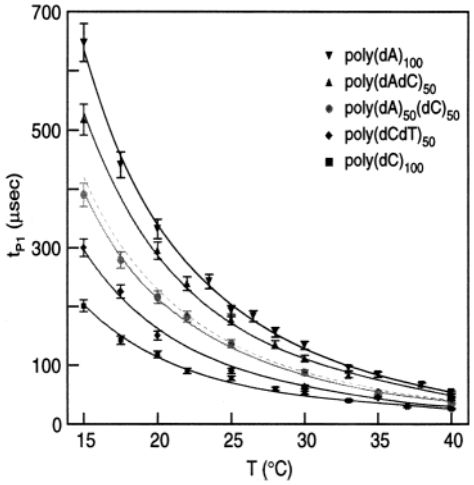

FIGURE 10. Dependence of blockade duration on temperature for poly(dA)$_{100}$, poly(dC)$_{100}$, poly(dA$_{50}$dC$_{50}$), poly(dAdC)$_{50}$, and poly(dCdT)$_{50}$. All measurements were performed at 120 mV. The dotted black line that matches closely to the poly(dA$_{50}$dC$_{50}$) data is the algebraic average of poly(dA)$_{100}$ and poly(dC)$_{100}$ (from Meller et al.[13]).

Temperature Effects on Nucleic Acid Translocation

To gain a better understanding of why different polymers translocate through the nanopore at different rates, we performed an extensive series of measurements from 15 to 40 °C with five polymer types: poly(dA)$_{100}$, poly(dC)$_{100}$, poly(dA$_{50}$dC$_{50}$), poly(dAdC)$_{50}$, and poly(dCdT)$_{50}$ (Figure 10). For all of the polymers tested, the temperature dependence for the translocation times, t_P, was best approximated by $\sim a/T^2 + b$ (full lines in Figure 10), where a is a constant that depends on the polymer type, T is the temperature in °C, and b is an additive constant. This relationship between translocation duration and T^{-2}, as well as an examination of Figure 10, makes it clear that at high temperatures, the differences in translocation rates between polymers will be diminished. For example, poly(dC)$_{100}$ was 3.2 times faster than poly(dA)$_{100}$ at 15 °C, but only 2.1 times faster at 40 °C. Further experiments at higher temperatures will be needed to determine whether all polymers approach a common value. If so, translocation through a nanopore could be used as a rapid measure of polymer length regardless of the polynucleotide's composition or sequence. Conversely, at low temperatures the differences between polymers are striking. This implies that experiments at 15 °C or lower will optimize the identification of individual polymers in a mixed population. For example, experiments at low temperatures demonstrate that as few as 10 substitutions of thymines within a 100-nucleotide poly(dC) polymer are readily detectable (unpublished data). Thus, at low temperatures, nanopore measurements are highly sensitive to replacements of one purine (cytosine) with another purine (thymine).

The strong temperature dependence of t_{P1} probably arises from a complex set of factors affecting both those portions of the polymer that are in the channel and those that are outside of the channel. The T^{-2} temperature

dependence for the translocation rate cannot be accounted for alone by changes in the viscosity of the medium, since these changes would contribute only a factor of T^{-1}. The discovery of a T^{-2} scaling should help to estimate the contribution of factors other than drag forces to the translocation rate.

Force Acting on Nucleic Acid Molecule

Force is a fundamental property of any electrophoretic system, including gel and single-pore electrophoresis of nucleic acids. We can estimate the driving force on the molecule[20] from $F \approx zeV/a$, where z is the effective charge per base, e is an elementary unit charge, V is the electrostatic potential drop through the pore, and a is the base-to-base distance along the DNA polymer. Assuming $z = 1$, $V = 125$ mV, and $a = 4$ Å, the force is estimated to be $F \approx 5k_BT/a \approx 44$ pN. If electrostatic shielding within the nanopore is similar to that in bulk solution,[27] shielding would be expected to reduce the full charge on the strand by a factor of ~0.45. Thus, the force may be closer to 20 pN. We would therefore predict that the force exerted on a DNA strand by a 125 mV bias is sufficient to overcome the entropic barrier due to the loose, random configurations of a DNA strand in bulk solution.[10] Indeed, for single-stranded poly dA at 2 °C, Meller et al.[20] found that a force of <17 pN was sufficient to overcome both the entropic barrier and the potential enthalpic barrier that would be created by any stacking of the adenine bases. We would also expect that a force around 20 pN would be just sufficient to break extensive hydrogen bonding that stabilizes base pairing. The experiments with hairpin loops described above confirm this expectation.

Synthetic Nanopores for Analyzing Nucleic Acids

We are now exploring synthetic nanopores that could have the potential to match or surpass α-hemolysin in detecting and analyzing nucleic acids in solution. In contrast to a labile protein in a delicate lipid bilayer, solid-state nanopores will be mechanically robust, tolerate a broad range of temperatures, pH, and chemical conditions, and provide a low-capacitance, low-noise surface suitable for integrated electronics. Ideally, the fabrication process used to make the solid-state nanopore should make it possible to easily control and vary pore dimensions so that these dimensions can be optimized for a particular application, e.g., probing single-stranded vs double-stranded DNA.

Fulfilling these requirements is difficult because fabrication methods able to manipulate matter at 10^{-9} m dimensions have not been available. For example, single 3−5 nm holes in an insulating silicon nitride membrane can be made using an erosion process, such as reactive ion etching,[28] but we found that this method produced nanopores with a range of dimensions from 3 to 40 nm, only a few of which were of the desired dimension. Achieving greater reproducibility requires knowing precisely when to stop the erosion process. One approach that can reproducibly fabricate nanopores of a desired dimension is a feedback-controlled ion-sputtering system that counts the ions transmitted through the gradually opening pore and extinguishes the ion-sputtering erosion process at the appropriate time.[29] With feedback control, reproducibility does not depend on precisely matching all conditions and starting dimensions. Using this system, we have been able to routinely produce robust single nanopores with 2, 3, or 4 nm diameters. Although many of these solid-state nanopores are electrically noisy, we are learning how to control this unwanted noise. For instance, we have recently shown that these nanopores are capable of registering translocation of single DNA molecules that produce characteristic curent blockade signals in much the same way as they do in the α-hemolysin pore.[29]

The ability to detect and identify single polymer molecules in solution has numerous applications, and these will be realized if a stable inorganic nanopore can be developed. Examples include measurement of nucleic acid concentration, for instance, during PCR amplification. It also seems reasonable to think that a synthetic nanopore in the size range of 4−6 nm diameter will be able to detect and perhaps identify individual soluble protein molecules. Hybridized DNA should be readily distinguished from single-stranded DNA by a nanopore of appropriate size, thus providing an alternative to microarrays for assays based on hybridization. Finally, the results to date have made it clear that a nanopore can resolve differences of single base pairs in DNA hairpins. It now seems feasible that a small increment in resolving power, coupled with controlled motion of a DNA strand through a nanopore, will permit single-molecule sequencing of nucleic acids.

This brief account of our research cannot be an exhaustive review of the literature related to nanopores and this burgeoning field. In particular, we would have liked to cite and discuss the work of Hagan Bayley, Sergey Bezrukov, Adrian Parsegian, and John Kasianowicz, who pioneered many of the methods and concepts now used. We particularly thank Mark Akeson, Eric Brandin, Amit Meller, and Wenonah Vercoutere for their superb research efforts in our laboratories. We also thank our colleague Jene Golovchenko for his contributions to the development of synthetic nanopores. Most of the research described here was sponsored by grants from NIH, DARPA, and NSF. Portions of this Account were adapted from Akeson et al.[8] and Vercoutere et al.[14]

References

(1) Henry, J.-P.; Chich, J.-F.; Goldschmidt, D.; Thieffry, M. Blockade of a mitochondrial cationic channel by an addressing peptide: An electrophysiological study. *J. Membr. Biol.* **1989**, *112*, 139−147.
(2) Bayley, H. Triggers and switches in a self-assembling pore-forming protein. *J. Cell. Biochem.* **1994**, *56*, 177−182.
(3) Bezrukov, S. M.; Vodyanoy, I.; Parsegian, V. A. Counting polymers moving through a single ion channel. *Nature* **1994**, *370*, 279−281.
(4) Bezrukov, S. M.; Vodyanoy, I.; Brutyan, R. A.; Kasianowicz, J. J. Dynamics and free energy of polymers partitioning into a nanoscale pore. *Macromolecules* **1996**, *29*, 8517−8522.
(5) Bustamante, J. O.; Oberleithner, H.; Hanover, J. A.; Liepins, A. Patch clamp detection of transcription factor translocation along the nuclear pore complex channel. *J. Membr. Biol.* **1995**, *146*, 253−261.
(6) Kasianowicz, J.; Brandin, E.; Branton, D.; Deamer, D. W. Characterization of individual polynucleotide molecules using a membrane channel. *Proc. Natl. Acad. Sci. U.S.A.* **1996**, *93*, 13770−13773.

(7) Braha, O.; Walker, B.; Cheley, S.; Kasianowicz, J.; Song, L.; Gouaux, J. E.; Bayley, H. Designed protein pores as components for biosensors. *Chem. Biol. (London)* **1997**, *4*, 497−505.
(8) Akeson, M.; Branton, D.; Kasianowicz, J. J.; Brandin, E.; Deamer, D. W. Microsecond time-scale discrimination among polycytidylic acid, polyadenylic acid, and polyuridylic acid as homopolymers or as segments within single RNA molecules. *Biophys. J.* **1999**, *77*, 3227−3233.
(9) Lubensky, D. K.; Nelson, D. R. Driven polymer translocation through a narrow pore. *Biophys. J.* **1999**, *77*, 1824−1838.
(10) Muthukumar, M. Polymer translocation through a hole. *J. Chem. Phys.* **1999**, *111*, 10371−10374.
(11) Bayley, H.; Braha, O.; Gu, L. Q. Stochastic sensing with protein pores. *Adv. Mater.* **2000**, *12*, 139−142.
(12) Gu, L. Q.; Bayley, H. Interaction of the noncovalent molecular adapter, beta-cyclodextrin, with the staphylococcal alpha-hemolysin pore. *Biophys. J.* **2000**, *79*, 1967−1975.
(13) Meller, A.; Nivon, L.; Brandin, E.; Golovchenko, J.; Branton, D. Rapid nanopore discrimination between single polynucleotide molecules. *Proc. Natl. Acad. Sci. U.S.A.* **2000**, *97*, 1079−1084.
(14) Vercoutere, W.; Winters-Hilt, S.; Olsen, H.; Deamer, D. W.; Haussler, D.; Akeson, M. Rapid discrimination among individual DNA molecules at single nucleotide resolution using a nanopore instrument. *Nat. Biotechnol.* **2001**, *19*, 248−250.
(15) Howorka, S.; Cheley, S.; Bayley, H. Sequence specific detection of individual DNA strands using engineered nanopores. *Nat. Biotechnol.* **2001**, *19*, 636−639.
(16) Davis, L. G.; Kuehl, W. M.; Battey, J. F. *Basic Methods in Molecular Biology*, 2nd ed.; Appleton and Lange: Norwalk, CT, 1994.
(17) Cantor, C. R.; Schimmel, P. R. *Biophysical Chemistry, Part III: The Behavior of Biological Macromolecules*; W. H. Freeman: San Francisco, 1980.
(18) Saenger, W.; Riecke, J.; Suck, D. A structural model for the polyadenylic acid single helix. *J. Mol. Biol.* **1975**, *93*, 529−534.
(19) Song, L.; Hobaugh, M. R.; Shustak, C.; Cheley, S.; Bayley, H.; Gouaux, J. E. Structure of Staphylococcal a-hemolysin, a heptameric transmembrane pore. *Science* **1996**, *274*, 1859−1866.
(20) Meller, A.; Nivon, L.; Branton, D. Voltage-driven DNA translocations through a nanopore. *Phys. Rev. Lett.* **2001**, *86*, 3435−3438.
(21) DeBlois, R. W.; Bean, C. P. Counting and sizing of submicron particles by the resistive pulse technique. *Rev. Sci. Instrum.* **1970**, *41*, 909−916.
(22) DeBlois, R. W.; Bean, C. P.; Wesley, R. K. A. Electrokinetic measurements with submicron particles and pores by the resistive pulse technique. *J. Colloid Interface Sci.* **1977**, *61*, 323−335.
(23) Erie, D. A.; Suri, A. K.; Breslauer, K. J.; Jones, R. A.; Olson, W. K. Theoretical predictions of DNA hairpin loop conformations: Correlations with thermodynamics and spectroscopic data. *Biochemistry* **1993**, *32*, 436−454.
(24) Antao, V P.; Tinoco, I., Jr. Thermodynamic parameters for loop formation in RNA and DNA hairpin tetraloops. *Nucleic Acids Res.* **1992**, *20*, 819−824.
(25) Rentzeperis, D.; Alessi, K.; Marky, L. A. Thermodynamics of DNA hairpins: contribution of loop size to hairpin stability and ethidium bromide. *Nucleic Acids Res.* **1993**, *21*, 2683−2689.
(26) Senior, M. M.; Jones, R. A.; Breslauer, K. J. Influence of loop residues on the relative stabilities of DNA hairpin structures. *Proc. Natl. Acad. Sci. U.S.A.* **1988**, *85*, 6242−6246.
(27) Manning, G. S. The molecular theory of polyelectrolyte solutions with applications to the electrostatic properties of polynucleotides. *Q. Rev. Biophys.* **1978**, *11*, 179−246.
(28) Ralph, D. C.; Black, C. T.; Tinkham, M. Spectroscopic measurements of discrete electronic states in single metal particles. *Phys. Rev. Lett.* **1995**, *74*, 3241−3244.
(29) Li, J.; Stein, D.; McMullan, C.; Branton, D.; Aziz, M. J.; Golovchenko, J. A. Ion-beam sculpting at nanometre length scales. *Nature* **2001**, *412*, 166−169.

AR000138M